Journal of Medicinal Chemistry

ARTICLE

pubs.acs.org/jmc

Design and Optimization of Potent and Orally Bioavailable Tetrahydronaphthalene Raf Inhibitors

Alexandra E. Gould,*[,†] Ruth Adams,[†] Sharmila Adhikari,[†] Kathleen Aertgeerts,[‡] Roushan Afroze,[†] Christopher Blackburn,[†] Emily F. Calderwood,[†] Ryan Chau,[†] Jouhara Chouitar,[†] Matthew O. Duffey,[†] Dylan B. England,[†] Cheryl Farrer,[†] Nancy Forsyth,[†] Khristofer Garcia,[†] Jeffery Gaulin,[†] Paul D. Greenspan,[†] Ribo Guo,[†] Sean J. Harrison,[†] Shih-Chung Huang,[†] Natalia Iartchouk,[†] Dave Janowick,[†] Mi-Sook Kim,[†] Bheemashankar Kulkarni,[†] Steven P. Langston,[†] Jane X. Liu,[†] Li-Ting Ma,[†] Saurabh Menon,[†] Hirotake Mizutani,[†] Erin Paske,[†] Christelle C. Renou,[†] Mansoureh Rezaei,[†] R. Scott Rowland,[†] Michael D. Sintchak,[†] Michael D. Smith,[†] Stephen G. Stroud,[†] Ming Tregay,[†] Yuan Tian,[†] Ole P. Veiby,[†] Tricia J. Vos,[†] Stepan Vyskocil,[†] Juliet Williams,[†] Tianlin Xu,[†] Johnny J. Yang,[†] Jason Yano,[‡] Hongbo Zeng,[†] Dong Mei Zhang,[†] Qin Zhang,[†] and Katherine M. Galvin[†]

[†]Millennium Pharmaceuticals, Inc., 40 Landsdowne Street, Cambridge, Massachusetts 02139, United States

[‡]Takeda San Diego, 10410 Science Center Drive, San Diego, California 92130, United States

Supporting Information

ABSTRACT: Inhibition of mutant B-Raf signaling, through either direct inhibition of the enzyme or inhibition of MEK, the direct substrate of Raf, has been demonstrated preclinically to inhibit tumor growth. Very recently, treatment of B-Raf mutant melanoma patients with a selective B-Raf inhibitor has resulted in promising preliminary evidence of antitumor activity. This article describes the design and optimization of tetrahydronaphthalene-derived compounds as potent inhibitors of the Raf pathway in vitro and in vivo. These compounds possess good pharmacokinetic properties in rodents and inhibit B-Raf mutant tumor growth in mouse xenograft models.

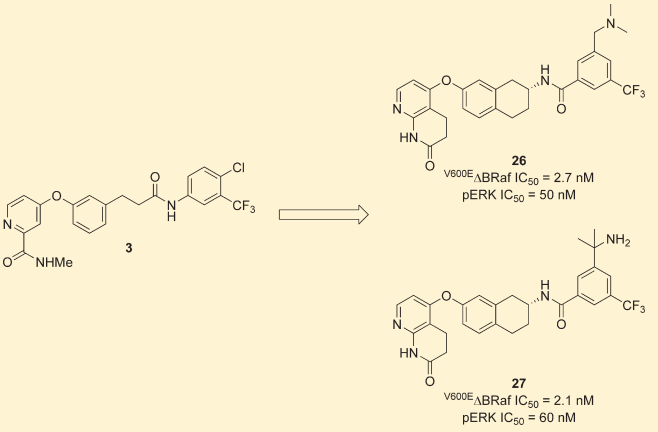

INTRODUCTION

The mitogen-activated protein kinase (MAPK) signal transduction pathway regulates cellular growth, proliferation, and differentiation in response to many different external stimuli.[1] This pathway is also frequently mutated in many types of cancer and thus contains attractive targets for oncology drug discovery.[2] One component of this pathway, the Raf isoform B-Raf, has a high rate of activating mutation in melanoma (50−70%) and other cancers including papillary thyroid (49%), colorectal (∼15%), and ovarian (∼30%).[3,4] The V600E activating mutation is most common and significantly increases the basal level activity of the enzyme.[5] Inhibition of mutant B-Raf signaling, through either direct inhibition of the enzyme[6] or inhibition of MEK, the direct substrate of Raf,[7] has been demonstrated preclinically to inhibit tumor growth. Very recently, treatment of B-Raf mutant melanoma patients with a selective B-Raf inhibitor has resulted in antitumor activity.[8]

At the time we began our work, sorafenib (**1**) was the only compound with known Raf activity in the clinic. Sorafenib is reported to have a reasonable enzyme potency against ^{V600E}ΔB-Raf and C-Raf (IC_{50} values of 38 and 6 nM, respectively) and pathway inhibition in cells (IC_{50} values of 40−1200 nM depending on the cell line).[9] We took the sorafenib scaffold as a starting point for our efforts and sought to identify compounds that display robust Raf pathway inhibition in an in vitro and in vivo setting. In this paper, we report the optimization of a series of novel tetrahydronaphthalene-derived compounds with respect to cellular activity and pharmacokinetic (PK) properties. In addition, these compounds profoundly inhibit both tumor growth and markers of Raf pathway activity in B-Raf mutant melanoma xenografts.

Received: November 17, 2010
Published: February 22, 2011

Scheme 1. Synthesis of Amide-Based Raf Inhibitors[a]

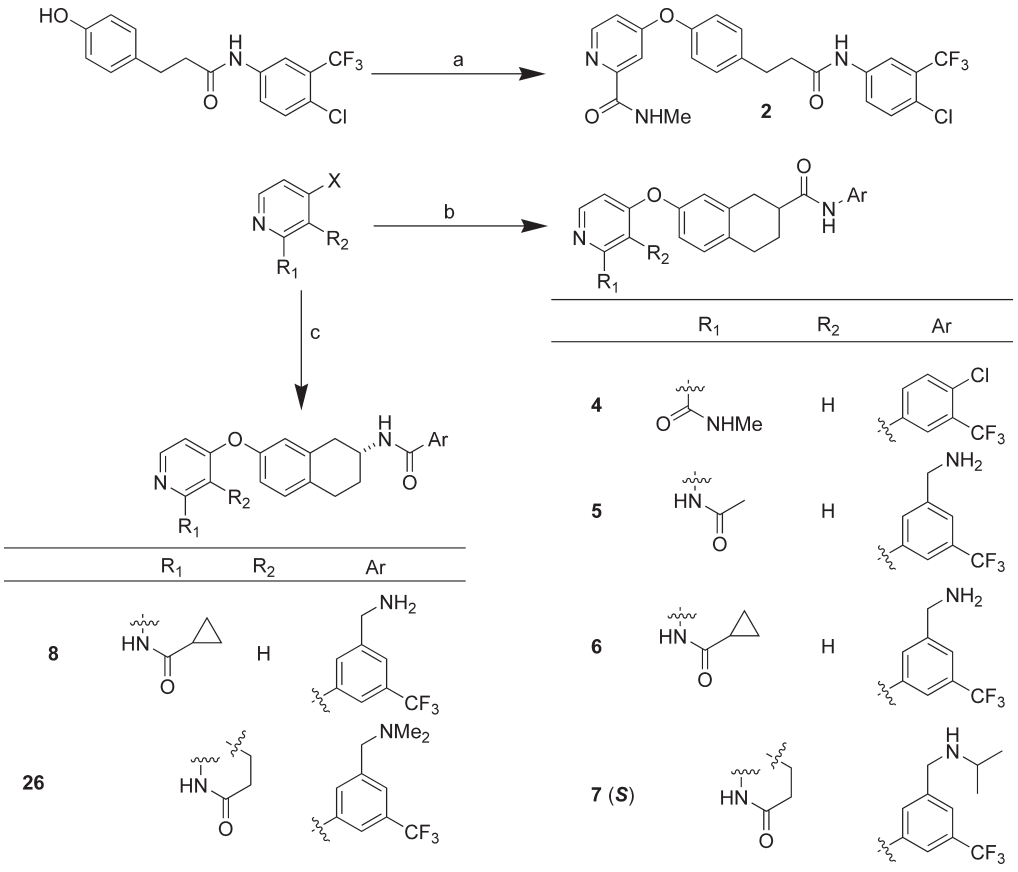

[a] Reagents and conditions: (a) 4-Chloro-*N*-methylpicolinamide, KOtBu, DMPU, DMF, 100 °C. (b) (±)-**15** or (*S*)-**15**, Cs_2CO_3, DMF, heat and then amide coupling. (c) Compound **17**, Cs_2CO_3, DMF, heat and then amide coupling.

Scheme 2. Synthesis of 4-Fluoropyridine Lactam[a]

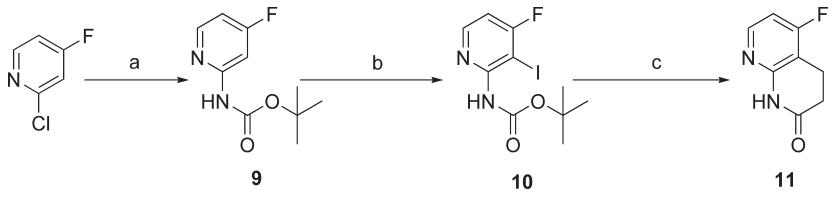

[a] Reagents and conditions: (a) *t*-Butyl carbamate, $Pd(OAc)_2$, Xantphos, NaOH, H_2O, dioxane, 80%. (b) *n*-BuLi, TMEDA, THF, −78 °C and then I_2, 86%. (c) Pd catalyst **29**, 3,3-diethoxy-1-propene, DIPEA, H_2O, DMF, 140 °C, 47%.

CHEMISTRY

We devised two modular approaches to the synthesis of the compounds of interest as shown in Scheme 1. The appropriately substituted aniline is coupled with a phenylpropionic acid. The resulting propanamide phenol and a substituted pyridine are heated in the presence of a base to provide a biaryl ether (e.g., **2**, Scheme 1). Alternatively, the biaryl ether bond is formed first when the appropriately substituted pyridine and phenol are heated in the presence of cesium carbonate. These biaryl ethers are then further reacted with either an aniline or a benzoic acid derivative to provide the desired compounds (e.g., **4** and **8**, Scheme 1).

The syntheses of several substituted pyridines such as 4-chloro-*N*-methylpicolinamide,[10] *N*-(4-nitropyridin-2-yl)acetamide, and cyclopropylacetamide[11] are described in the literature. Pyridine lactam **11** is prepared in three steps from 2-chloro-4-fluoropyridine (Scheme 2). Palladium-catalyzed amination provides the Boc-protected aminopyridine (**9**). ortho-Lithiation and iodination set the stage for a one-pot palladium-catalyzed Heck coupling/cyclization to provide lactam **11** (Scheme 2) in modest yield.

The synthesis of the (*S*)-tetrahydronaphthalene carboxylic acid (*S*)-**15** (Scheme 3) begins with the Evans' oxazolidinone amide of phenylpropionic acid (**12**). Asymmetric alkylation of this oxazolidinone with *t*-butyl bromoacetate proceeds with high diastereoselectivity to provide **13** in good yield.[12] Deprotection of the *t*-butyl ester, Friedel−Crafts cyclization,[13] and removal of the oxazolidinone gives tetralone acid **14**. Subsequent reduction of the tetralone and deprotection of the methyl ether with BBr_3 affords the desired tetrahydronaphthalene carboxylic acid (*S*)-**15**

dx.doi.org/10.1021/jm101479y |*J. Med. Chem.* 2011, 54, 1836–1846

Scheme 3. Synthesis of *S*-Tetrahydronaphthalene Carboxylic Acid[a]

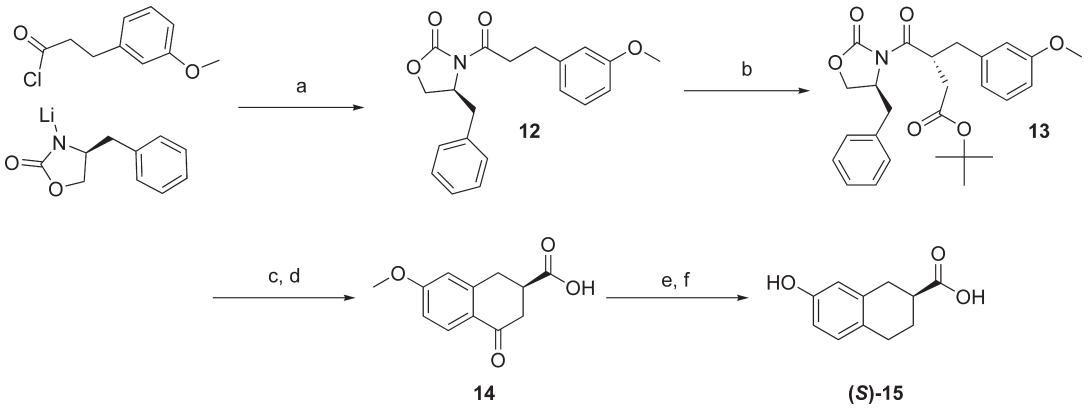

[a] Reagents and conditions: (a) THF, −78 °C, 89%. (b) NaHMDS, THF −78 °C and then *t*-butyl bromoacetate, 79%. (c) CF_3SO_3H, PhH, 80 °C, o/n. (d) H_2O_2, NaOH, THF 0 °C, 70% for two steps. (e) Pd/C, H_2, H_2SO_4, AcOH, 80 °C, 20 psi, 65%. (f) BBr_3, DCM, −78 to 0 °C, 74%.

Scheme 4. Synthesis of Amino Tetrahydronaphthalene[a]

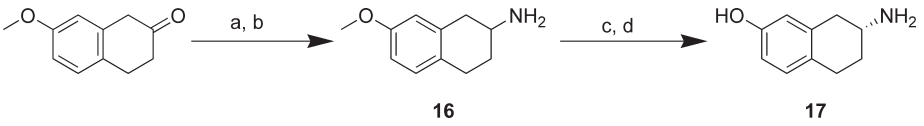

[a] Reagents and conditions: (a) $BnNH_2$, $NaBH(OAc)_3$, AcOH, DCM, 100%. (b) $Pd(OH)_2$, H_2, EtOH, AcOH, 92%. (c) NaOH, EtOAc, 92% and then *S*-(+)-mandelic acid, iPrOH, MeOH, H_2O, PhMe, 60%. (d) HBr, H_2O, reflux, 99%.

in good yield while maintaining enantiopurity. Careful control of the methyl ether deprotection reaction conditions was crucial as this substrate was prone to racemization, particularly on scale.[14]

To prepare the single enantiomer aminotetralin **17** (Scheme 4), we modified a procedure described in the patent literature.[15] Reductive amination of 7-methoxy-2-tetralone and benzyl amine followed by debenzylation provides 7-methoxy-2-aminotetralin (**16**). Crystallization of the free base of the aminotetralin **16** with (*S*)-mandelic acid using slightly modified solvents to those previously reported,[16] followed by HBr deprotection of the methyl ether, provides the desired tetralin amine **17** in high ee and good yield.

RESULTS AND DISCUSSION

An examination of the crystal structure of sorafenib bound to ^{V600E}ΔB-Raf[17] reveals several important features that contribute to the potency of the molecule as it occupies the ATP binding site of the enzyme in its DFG-out conformation. The pyridine ring makes key contacts in the hinge region of the enzyme. The trifluoromethyl group on the phenyl ring occupies a hydrophobic pocket formed by regions of the DFG motif and the catalytic loop of the enzyme, while the urea forms two hydrogen bonds with the enzyme. We decided to explore the importance of these two hydrogen bonds by replacing the urea with a variety of alternative moieties and quickly identified **2** (Table 1) in which the urea of sorafenib has been replaced with a propionamide. The enzyme tolerates the increase in chain length as well as the loss of one of the hydrogen bond donor groups of the urea. Both meta- and para-substituted molecules are acceptable (**2** and **3**, Table 1) and have similar potency against both ^{V600E}ΔB-Raf and C-Raf.

Although these compounds were quite potent in our enzyme assays, they did not show any activity in a cellular assay measuring

Table 1. Sorafenib and Initial Amide-Based Raf Inhibitors

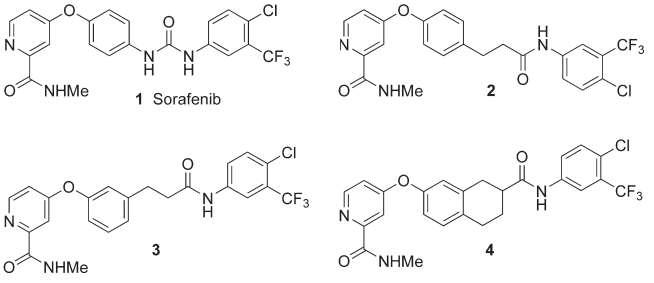

	^{V600E}ΔB-Raf IC_{50} (nM)[a]	C-Raf IC_{50} (nM)[a]	pERK IC_{50} (nM)[a]
2	61 ± 11	10 ± 2	>25000[c]
3	47 ± 12	9 ± 2	>25000[c]
4	32[b]	28[b]	2900[b]

[a] IC_{50} values are shown as mean values of three or more determinations. [b] IC_{50} values are shown as mean of two determinations. [c] IC_{50} values are shown as single determinations.

inhibition of extracellular signal-regulated kinase (ERK) kinase phosphorylation (pERK) in A375 cells (a melanoma cell line that contains ^{V600E}ΔB-Raf). Constraint of the flexible central core of compound **3** (Table 1) through cyclization did not improve the enzyme activity but did improve cellular activity, as tetralin **4** (Table 1), prepared as a racemic mixture, now has cellular activity in the low micromolar range.

Having identified a series of novel compounds with modest cellular activity, we next focused on improving the cellular potency of the series while keeping a close eye on the

dx.doi.org/10.1021/jm101479y |*J. Med. Chem.* 2011, 54, 1836–1846

Table 2. Enzyme and Cellular Potencies of Raf Inhibitors

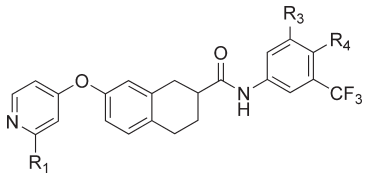

	R_1	R_3	R_4	$^{V600E}\Delta$B-Raf IC_{50} (nM)[a]	C-Raf IC_{50} (nM)[a]	pERK IC_{50} (nM)[a]
4		H	Cl	32[b]	28[b]	2,900[b]
18		H	CH_2NH_2	26 ± 8	16 ± 5	5,000 ± 3,000
19		CH_2NH_2	H	20 ± 12	11 ± 5	1,400 ± 500
5		CH_2NH_2	H	7 ± 2	6.0 ± 0.8	150 ± 58
6		CH_2NH_2	H	8 ±1	6.2 ± 0.6	150[b]
20 (*S*)		CH_2NH_2	H	5.0[b]	4.5[b]	130[b]
21(*R*)		CH_2NH_2	H	6.0[b]	6[b]	780[b]
22 (*S*)		CH_2NMe_2	H	4 ± 1	3.3 ± 0.9	130 ± 26
23		CH_2NH*i*-Pr	H	5.0 ± 0.5	4.6 ± 0.8	190 ± 42

[a] IC_{50} values are shown as mean values of three or more determinations. [b] IC_{50} values are shown as mean of two determinations.

physicochemical and PK behavior of the molecules. Introduction of a basic amine to the aryl amide portion of the molecule was evaluated as a means of improving the aqueous solubility of the series. Replacement of the 4-chloro substituent with a primary benzyl amine at either the 4- or the 5-position of the phenyl ring (**18** and **19**, respectively, Table 2) was tolerated, although this modification did not improve inhibitory activity in the enzyme or cellular assays.

Major improvements in enzyme and cellular activity were observed with alteration of the substituent on the pyridine ring, the hinge-binding element of the series. A simple reversal of the pyridine amide moiety (which is expected to maintain this interaction) provided a 10-fold improvement in cellular potency (cf. **19** and **5**, Table 2). A cyclopropyl amide (compound **6**) was also well tolerated, but more sterically demanding amides (e.g., isobutyryl or pivaloyl) led to decreases in cellular and enzyme activity (compounds and data not shown).

The enantiomers of **6** were separated by chiral HPLC, and the absolute stereochemistry was subsequently confirmed by synthesis of the individual enantiomers. While the enzyme activity of these two antipodes is quite similar, (*S*)-enantiomer **20** (Table 2) appears to be somewhat more potent in a cellular setting.

Amine **6** is a potent inhibitor of Raf in cells, but it has some significant PK liabilities. While the compound has low in vivo clearance (Table 3), it exhibits poor oral exposure and bioavailability in rats. In an effort to improve the PK properties, we focused on two areas of the molecule, the benzylic amine and the pyridine amide moiety. Exploration of the amine moiety revealed that various secondary and tertiary benzyl amines are all potent inhibitors of Raf. Dimethylation of the primary benzyl amine of **6** provided tertiary amine **22**, which maintained good potency and demonstrated improved oral exposures (Table 3); the isopropyl benzyl amine **23** also showed good cellular potency (Table 2) and significantly improved oral exposures in a rat PK experiment (Table 3, discrete rat IV data were not obtained for this molecule). Efforts to replace the amide substituent on the pyridine with a variety of heterocycles did not lead to compounds with an acceptable combination of cellular activity and in vivo clearance. As mentioned above, more sterically demanding amides were not well tolerated, but cyclization of the amide to a lactam provided potent compounds with improved oral exposures. A combination of the lactam and isopropyl benzyl amine in one molecule yielded **7** as one of our better compounds with respect to potency, in vivo clearance, and oral exposure (Table 3).

Continued optimization and exploration of the series led us to examine the effect of reversing the internal amide in this series. As exemplified by compound **8**, this modification appeared to have little impact on either the potency or the PK properties of the molecule (Table 3). Interestingly, the more potent enantiomer (**8**, *R*) with this amide bond orientation has the opposite stereochemistry when compared to the more potent enantiomer in the opposite amide bond orientation (**22**, *S*).

Because of the straightforward nature of the synthesis of the aminotetralin template required for this subseries, as well as the lack of a risk of racemization (which was occasionally observed in the synthesis of molecules related to compound **7**), the focus of our efforts now shifted to optimizing compound **8**. We were able to apply what we had learned from the optimization of the initial tetralin scaffold to improve the PK properties of this subseries and quickly identified **26** (ML721)[18] as a molecule with excellent cellular potency and PK properties (Table 3).

Significant demethylation of **26** to the monomethyl benzyl amine **28** was observed in vivo, and this metabolite was generally found to be present at ~30% of the circulating levels of **26** after oral dosing, as measured by area under the curve (AUC). We investigated **28** as a potential substitute for **26** and found that it did not perform as well as desired in vivo either in rat PK studies (see Table 3) or in mouse PK/pharmacodynamic (PD) studies (data not shown). A variety of substituted benzyl amines (as well as other amine-containing moieties) were explored, and we identified **27** (ML786)[18] as a molecule that maintained good cellular potency and acceptable PK properties but did not form any known active metabolites in vivo.

Both of these compounds, **26** and **27**, were found to have activity in vivo. As can be seen from Table 4, both compounds strongly inhibit the Raf pathway in vivo following a 75 or 100 mg/kg oral dose. As a class, these compounds have been found to inhibit a significant number of kinases (Table 5)[19] and are inhibitors of wild-type B-Raf and C-Raf. Although **26** and **27** display significant receptor tyrosine kinase activity, we were confident that this additional activity would not contribute significantly to pERK inhibition in melanoma tumors with constituitively activated B-Raf. This hypothesis was confirmed

Table 3. Structures, Raf Potency, and Rrat PK Parameters for Key Raf Inhibitors

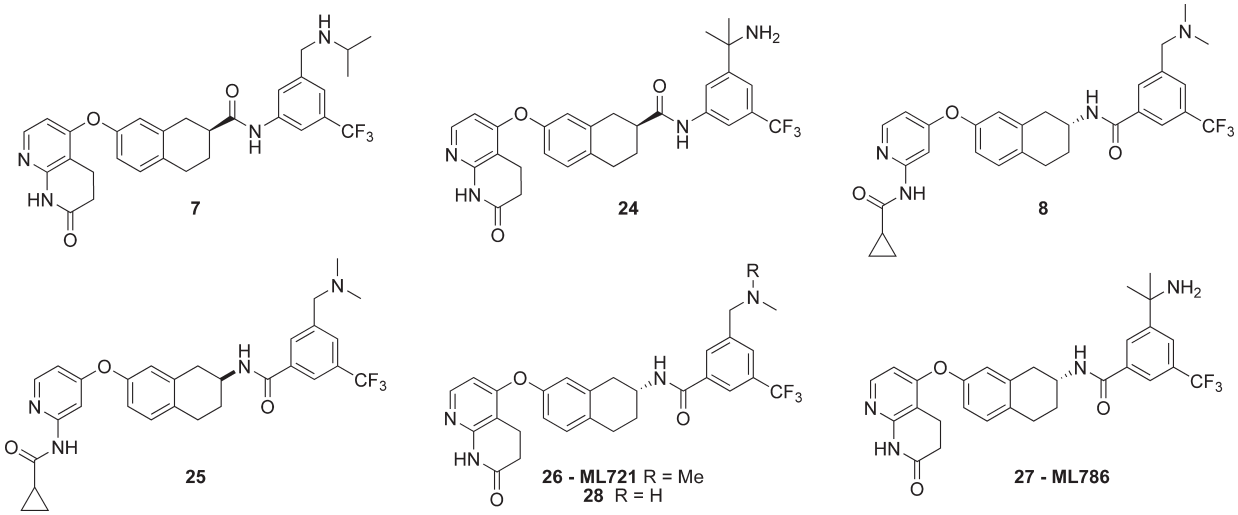

	^{V600E}ΔB-Raf IC_{50} (nM)[a]	pERK IC_{50} (nM)[a]	Clp (L/h/kg)[c]	Vss (L/kg)[c]	po AUC_{1-24h} (μM h)[c]	po % F[c]
6	8 ± 1	150[b]	0.4[d]	6.4	0.58[d]	1.9
22	4 ± 1	130 ± 26	1.41[d]	6.07	2.87[d]	27
23	5.0 ± 0.5	190 ± 42	ND[e]	ND	15.6[f]	ND
7	3.3 ± 0.3	110 ± 40	0.32	3.87	20.7	20
24	2.9[b]	79 ± 37	ND	ND	ND	ND
8	2.9 ± 0.5	70 ± 26	2.14	2.19	0.51	22
25	3.2 ± 0.2	1100[b]	ND	ND	ND	ND
26	2.7 ± 0.5	50 ± 26	0.23	0.75	98.6	100
27	2.1 ± 0.5	60 ± 30	0.44	3.93	35.9	85
28	2.2 ± 0.5	45 ± 11	0.73	4.01	12.4	50

[a] Unless otherwise noted, IC_{50} values are shown as mean values of three or more determinations. [b] IC_{50} values are shown as means of two determinations. [c] Average of three rats dosed at 1 mg/kg iv or 10 mg/kg po. Vehicle, 10% HPbCD. [d] Vehicle: po, 20% HPbCD; iv, PEG400/H_2O/EtOH/DMA (4:4:1:1). [e] ND, not determined. [f] Data from a single rat dosed at 10 mg/kg po. Vehicle, 20% HPbCD.

Table 4. Inhibition of pERK Formation In Vivo Following an Oral Dose of Select Raf Inhibitors[a]

	hours postdose	pERK (% inhibition)[d]	plasma concentration (μM)[e]
26	4[b]	93 ± 2	28 ± 7
	8[b]	92 ± 1	29 ± 5
	24[b]	72 ± 6	0.4 ± 0.1
27	4[c]	87 ± 4	23 ± 4
	8[c]	90 ± 2	27 ± 3
	24[c]	83 ± 7	3.0 ± 0.6

[a] PK/PD studies were performed in nude mice bearing A375 M xenografts. Compounds were dosed as solutions in 10% HPbCD. [b] Xenografts were harvested for analysis at the time listed after a single 100 mg/kg dose. [c] Xenografts were harvested for analysis at the time listed after a single 75 mg/kg dose. [d] Average of pERK levels determined by Li-Cor quantitative Western blots (3 or 4 animals per group) as compared to vehicle control set at 100%. [e] Average of compound levels in the plasma of mice determined by LC/MS/MS quantitation (3 or 4 animals per group).

Table 5. Selected Kinase Selectivity Data for 26 and 27[a]

IC_{50} (nM)	26	27
^{V600E}ΔB-Raf	2.7	2.1
wt B-Raf	4.7	4.2
C-Raf	2.2	2.5
Abl-1	1.2	<0.5
DDR2	2.6	7.0
EGFR	4900	190
EPHA2	18	11
KDR	59	6.2
LCK	610	170
MEK	>10000	1400
p38α	91	42
PDGFR	1100	47
RET	1.6	0.8

[a] IC_{50} values are shown as means of two determinations. ATP concentration for each kinase = K_{mapp}. Single-concentration binding data for 220 kinases can be found in the Supporting Information, Table 1.

with the observation that neither sunitinib [a multi-RTK (receptor tyrosine kinase)] nor erlotinib (an EGFR inhibitor) demonstrated significant pERK inhibition in A375 cells in a cellular setting or in A375 M tumors upon in vivo dosing (data not shown).

dx.doi.org/10.1021/jm101479y |J. Med. Chem. 2011, 54, 1836–1846

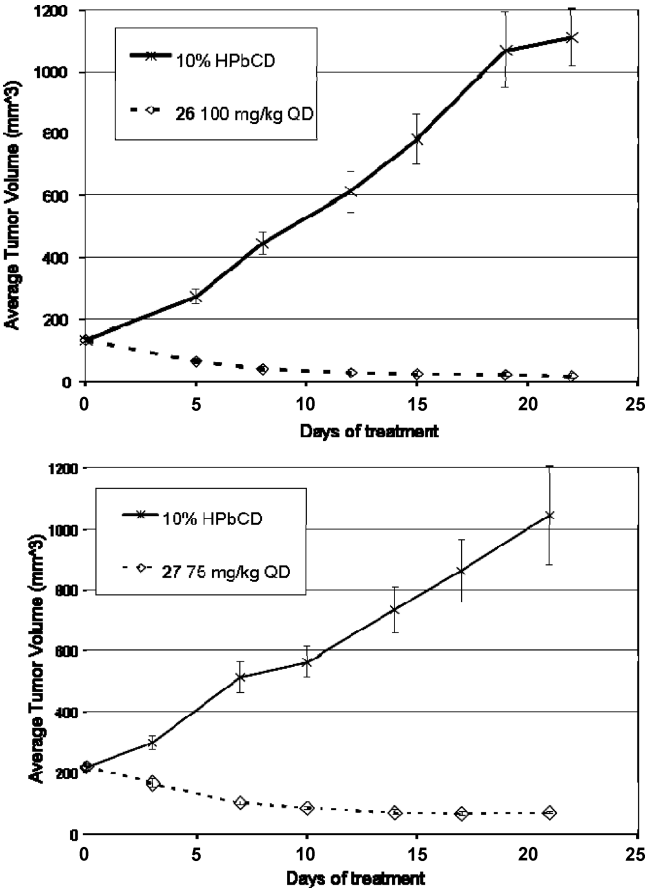

Figure 1. Inhibition of subcutaneous A375 M xenografts in immunocompromised mice by **26** and **27**. The doses shown are the maximum daily dose tolerated without body weight loss. Each compound was administered po/qd for 21 days.

Furthermore, once daily dosing for 21 days at 100 mg/kg for **26** or 75 mg/kg for **27** induces partial regressions of the tumor xenografts. These doses are well tolerated by the mice and show no indication of toxicity or weight loss as compared to vehicle-treated animals (Figure 1).

A crystal structure of a representative of this series, compound **24**, bound to the active site of wt B-Raf revealed the expected mode of binding to the DFG-out conformation (Figure 2). Key hinge contacts are achieved by the bicyclic pyridine lactam moiety nitrogens, the CF_3 substituent occupies a key hydrophobic pocket, and the central amide supplies a single hydrogen bond.[20]

We began our work searching for novel compounds that robustly inhibit the Raf pathway and demonstrate a strong antitumor effect in models of B-Raf mutant melanoma at well-tolerated doses. In identifying **26** and **27**, we have fulfilled that search. These molecules show potent inhibition of B-Raf in cells, possess excellent physicochemical and PK properties, potently inhibit the B-Raf pathway in mouse PK/PD studies, and show good efficacy in B-Raf mutant xenograft studies.

EXPERIMENTAL SECTION

NMR spectra were recorded in the solvent reported on a Bruker 300 MHz Avance1 or 400 MHz Avance2 (5 mm QnProbe) using residual solvent peaks as the reference. Compound purity was determined by analysis of the diode array UV trace of an LC-MS spectrum using the following procedure. Compounds were dissolved in DMSO, methanol, or acetonitrile, and the solutions were analyzed using an Agilent 1100 LC interfaced to a micromass Waters Micromass Zspray Mass Detector (ZMD). One of two gradients was used to elute the compounds either a formic acid (FA) gradient (acetonitrile containing 0−100% 0.1% formic acid in water) or an ammonium acetate (AA) gradient (acetonitrile containing 0−100% 10 mM ammonium acetate in water). All compounds were determined to be >95% pure unless otherwise noted. High-resolution mass spectra were recorded using a Thermo LTQ-FT Ultra mass spectrometer equipped with an Eksigent nanoLC Ultra system. About 500 pg of each compound was injected into an in-house packed reverse phase nanobore column (75 μm ID) with Magic C18 resin (Michrom BioResources, Auburn, CA) to a length of 12 cm. The pump flow rate was 300 nL/min. Buffer A is the aqueous solvent and consisted of 0.1% formic acid (Sigma, St. Louis, MO) in HPLC grade water (VWR Scientific, West Chester, PA). Buffer B, the organic phase, consisted of 0.1% formic acid in 90% acetonitrile (VWR Scientific) and 10% HPLC grade water. The gradient was set as follows: 0 min, 2% buffer B; 32 min, 42% buffer B; 35 min, 90% buffer B; and 36 min, 2% buffer B. The compounds were ionized using a New Objective PicoView Nanospray Source with 2.2 kV voltage. The mass spectrometer was set to acquire masses from 350 to 2000 D in positive mode. MS/MS spectra of each compound were also acquired under data-dependent acquisition mode to confirm the chemical structure of the compounds (data not shown).

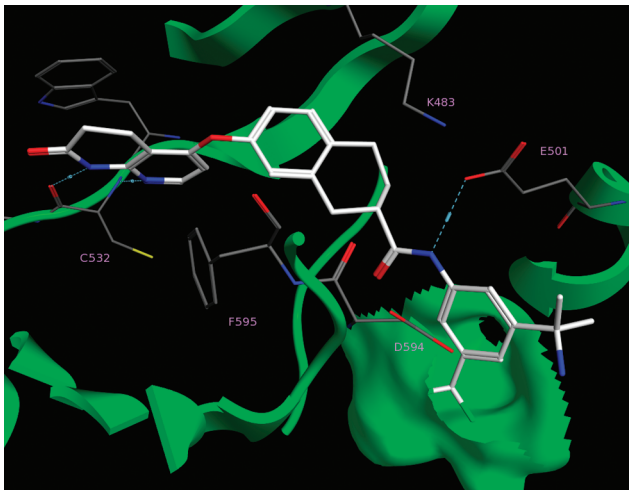

Figure 2. Crystal structure of **24** solved in complex with B-Raf (3.1 Å resolution).

4-[4-(3-{[4-Chloro-3-(trifluoromethyl)phenyl]amino}-3-oxopropyl)phenoxy]-*N*-methylpyridine-2-carboxamide (2). A mixture of 3-(4-hydroxyphenyl)propanoic acid (4 × 250 mg, 24.1 mmol total), 4-chloro-3-(trifluoromethyl)aniline (4 × 190 mg, 15.5 mmol total), and HATU (4 × 0.58 g, 24.1 mmol total) were added to four microwave-safe vials. To each vial, NMP (5 mL) and DIPEA (0.425 mL, 9.7 mmol) were added. The vials were then sealed and subjected to microwave irradiation at 220 °C for 15 min. The reaction vessels were unsealed, and the mixtures were combined and diluted with EtOAc. The organic solution was extracted with 1 N HCl and brine, dried over Na_2SO_4, filtered, and concentrated to give a brown oil. Purification by column chromatography (SiO_2, elution with EtOAc in hexane) provided *N*-[4-chloro-3-(trifluoromethyl)phenyl]-3-(4-hydroxyphenyl)propanamide as a yellow oil that solidified upon exposure to DCM (960 mg, 47% yield, ~95% pure). ^{1}H NMR (300 MHz, $CDCl_3$): δ 7.74 (br d, J = 2.4 Hz, 1H), 7.65 (br dd, J = 8.5 Hz, 2.3 Hz, 1H), 7.42 (d, J = 8.7 Hz, 1H), 7.16 (br s, 1H), 7.10 (d, J = 8.5 Hz, 2H), 6.79 (d, J = 8.5 Hz, 2H), 2.99 (t, J = 7.4 Hz, 2H), 2.65 (t, J = 7.4 Hz, 2H).

To a mixture of DMPU (0.7 mL) and DMF (2.8 mL) was added *N*-[4-chloro-3-(trifluoromethyl)phenyl]-3-(4-hydroxyphenyl)propanamide (600 mg, 1.75 mmol) and 4-chloro-N-methylpicolinamide[10] (328 mg, 1.92 mmol). To this solution was added KO^{t}Bu (590 mg, 5.25 mmol). The reaction mixture was stirred at 100 °C for 18 h and then cooled to room temperature, diluted with water, and extracted with EtOAc and DCM. The combined organic solutions were washed with water and brine, dried over Na_2SO_4, filtered, and concentrated to give a brown oil. Purification by column chromatography provided 4-[4-(3-{[4-chloro-3-(trifluoromethyl)phenyl]amino}-3-oxopropyl)phenoxy]-*N*-methylpyridine-2-carboxamide as a colorless solid (100 mg, 12% yield). ^{1}H NMR (300 MHz, CD_3OD): δ 10.11 (br s, 0.3H), 8.41 (d, J = 5.6 Hz, 1H), 8.07 (br d, J = 2.2 Hz, 1H), 7.74 (br dd, J = 8.7, 2.1 Hz, 1H), 7.48−7.51 (m, 2H), 7.36 (d, J = 8.5 Hz, 1H), 7.05 (d, J = 8.5 Hz, 2H), 6.98 (dd, J = 5.6, 2.5 Hz, 1H), 3.34 (s, 0.8H), 3.04 (t, J = 7.5 Hz, 2H), 2.92 (s, 3H), 2.71 (t, J = 7.5 Hz, 2H).

4-[3-(3-{[4-Chloro-3-(trifluoromethyl)phenyl]amino}-3-oxopropyl)phenoxy]-*N*-methylpyridine-2-carboxamide (3). A mixture of *N*-[4-chloro-3-(trifluoromethyl)phenyl]-3-(3-hydroxyphenyl)propanamide [585 mg, 1.70 mmol, prepared as described above using 3-(3-hydroxyphenyl)propanoic acid and 4-chloro-3-(trifluoromethyl)aniline], 4-chloro-*N*-methylpicolinamide[10] (318 mg, 1.87 mmol), and Cs_2CO_3 (7.76 g, 8.5 mmol) in DMF (3.4 mL) was heated at 100 °C overnight. The reaction mixture was concentrated and diluted with EtOAc. The organic solution was washed with brine, dried over $MgSO_4$, filtered, and concentrated. The residue was purified by column chromatography (SiO_2, 0−30% EtOAc in hexanes) to give **3** as a white solid (10 mg, 1% yield). ^{1}H NMR (400 MHz, CD_3OD): δ 8.39 (d, J = 5.58 Hz, 1H), 8.03 (d, J = 2.43 Hz, 1H), 7.74−7.66 (m, 1H), 7.50 (dd, J = 8.12, 5.65 Hz, 2H), 7.40 (d, J = 7.86 Hz, 1H), 7.22 (d, J = 7.68 Hz, 1H), 7.06 (s, 1H), 7.03−6.96 (m, 2H), 3.05 (t, J = 7.48, 7.48 Hz, 2H), 2.93 (s, 3H), and 2.71 (t, J = 7.46, 7.46 Hz, 2H). LCMS: m/z 478.3 $[M + H]^+$ (AA).

General Procedure A1, Biaryl Ether Bond Formation. A mixture of 7-hydroxy-1,2,3,4-tetrahydronaphthalene-2-carboxylic acid (8.00 g, 41.6 mmol), 4-chloro-*N*-methylpicolinamide[10] (8.58 g, 50.3 mmol), and cesium carbonate (40.7 g, 125 mmol) in DMF (150 mL) was heated at 100 °C overnight. The reaction was cooled to room temperature and concentrated under vacuum. The resulting slurry was diluted with water and acidified with 1 N HCl solution to pH 3. The mixture was allowed to stand at room temperature, and a precipitate formed. This precipitate was isolated by filtration, washed well with water, and thoroughly dried to give 7-({2-[(methylamino)carbonyl]pyridin-4-yl}oxy)-1,2,3,4-tetrahydronaphthalene-2-carboxylic acid as a white solid (12.10 g, 89%). ^{1}H NMR (400 MHz, d_6-DMSO): δ 8.48 (d, J = 5.6 Hz, 1H), 8.76 (d, J = 4.8 Hz, 1H), 12.30 (s, 1H), 7.35 (d, J = 2.6 Hz, 1H), 7.20 (d, J = 8.3 Hz, 1H), 7.13 (dd, J = 5.6, 2.6 Hz, 1H), 6.99 (d, J = 2.4 Hz, 1H), 6.94 (dd, J = 8.3, 2.6 Hz, 1H), 2.93 (d, J = 5.4 Hz, 1H), 2.83 (ddd, J = 9.4, 7.8, 3.6 Hz, 1H), 2.72 (s, 1H), 2.16−2.06 (m, 1H), and 1.81−1.68 (m, 1H).

4-{[7-({[4-Chloro-3-(trifluoromethyl)phenyl]amino}carbonyl)-5,6,7,8-tetrahydronaphthalen-2-yl]oxy}-*N*-methylpyridine-2-carboxamide (4). 4-Chloro-3-(trifluoromethyl)aniline (160 mg, 0.817 mmol), 7-({2-[(methylamino)carbonyl]pyridine-4-yl}oxy)-1,2,3,4-tetrahydronaphthalene-2-carboxylic acid (254 mg, 0.778 mmol), EDCI (149 mg, 0.778 mmol), and DMAP (114 mg, 0.943 mmol) were suspended in DCM (2.74 mL) in a microwave vial. The vial was sealed, and the reaction mixture was subjected to microwave irradiation at 60 °C for 5 min. Water and DCM were added to the reaction mixture, and the phases were separated. The organic phase was dried over $MgSO_4$, filtered, and concentrated. Purification by column chromatography (SiO_2, elution with 10−50% EtOAc in hexanes) provided 210 mg of desired product. This material was taken up in DCM and treated with 1 N HCl in Et_2O. The solution was concentrated to give the HCl salt of **4** as an off-white solid (175 mg, 42%). ^{1}H NMR (400 MHz, d_6-DMSO): δ 10.43 (s, 1H), 8.49 (d, J = 5.71 Hz, 1H), 8.21 (d, J = 2.48 Hz, 1H), 7.85 (dd, J = 8.81, 2.45 Hz, 1H), 7.61 (d, J = 8.83 Hz, 1H), 7.46 (d, J = 2.27 Hz, 1H), 7.23 (d, J = 8.30 Hz, 1H), 7.16 (dd, J = 5.73, 2.57 Hz, 1H), 6.99 (d, J = 2.39 Hz, 1H), 6.95 (dd, J = 8.23, 2.51 Hz, 1H), 3.01−2.92 (m, 2H), 2.91−2.72 (m, 6H), 2.19−2.06 (m, 1H), and 1.92−1.72 (m, 1H). LC-MS: m/z 504.3/506.3 $[M + H]^+$, 502.4/504.3 $[M - H]^-$ (AA). HRMS: m/z calcd for $C_{25}H_{22}N_3O_3ClF_3$ $([M + H])^+$, 504.12963; found, 504.130179.

General Procedure B1, Amide Bond Formation. 7-({2-[(Methylamino)carbonyl]pyridine-4-yl}oxy)-1,2,3,4-tetrahydronaphthalene-2-carboxylic acid (400 mg, 1.22 mmol), 5-amino-2-cyanobenzotrifluoride (251 mg, 1.35 mmol), EDCI (258 mg, 1.35 mmol), and DMAP (180 mg, 1.47 mmol) were combined in DCM (10 mL), and the resulting mixture was stirred overnight at room temperature. The reaction mixture was concentrated in vacuo, diluted with EtOAc, and extracted with aqueous 1 N HCl solution. The organic phase was washed with brine, dried over $MgSO_4$, filtered, and concentrated. Purification by column chromatography (SiO_2, elution with 0−50% EtOAc in hexanes) provided 4-{[7-({[4-cyano-3-(trifluoromethyl)phenyl]amino}carbonyl)-5,6,7,8-tetrahydronaphthalen-2-yl]oxy}-*N*-methylpyridine-2-carboxamide as a white powder (480 mg, 79%). ^{1}H NMR (400 MHz, $CDCl_3$): δ 9.30 (s, 1H), 8.33 (d, J = 5.6 Hz, 1H), 8.25−8.18 (m, 1H), 8.22 (d, J = 4.9 Hz, 1H), 8.11 (d, J = 1.8 Hz, 1H), 8.03 (dd, J = 8.5, 1.9 Hz, 1H), 7.73 (d, J = 8.5 Hz, 1H), 7.52 (d, J = 2.5 Hz, 1H), 7.06 (d, J = 8.3 Hz, 1H), 7.00 (dd, J = 5.6, 2.5 Hz, 1H), 6.81 (dd, J = 8.2, 2.3 Hz, 1H), 6.67 (d, J = 2.0 Hz, 1H), 3.05−2.97 (m, 4H), 2.88 (dd, J = 16.9, 3.4 Hz, 2H), 2.77−2.60 (m, 2H), 2.22−2.13 (m, 1H), and 2.01−1.89 (m, 1H).

4-{[7-({[4-(Aminomethyl)-3-(trifluoromethyl)phenyl]amino}carbonyl)-5,6,7,8-tetrahydronaphthalen-2-yl]oxy}-*N*-methylpyridine-2-carboxamide (18). 4-{[7-({[4-Cyano-3-(trifluoromethyl)phenyl]amino}carbonyl)-5,6,7,8-tetrahydronaphthalen-2-yl]oxy}-*N*-methylpyridine-2-carboxamide (200 mg, 0.4 mmol) was dissolved in 7.0 M NH_3 in MeOH solution. To this solution was added Raney 2800 nickel (50% v/v slurry in water, approx 2 mL), and the mixture was stirred under an atmosphere of hydrogen gas for 5 h. The reaction mixture was filtered through a pad of Celite, and the filtrate was concentrated. Purification by column chromatography [SiO_2, elution with 0−5% MeOH (with 1% NH_4OH) in DCM] provided **18** as a white solid. This material was taken up in DCM and treated with 1 N HCl in Et_2O. The solution was concentrated to give the HCl salt of **18** as a white solid (110 mg, 52%). ^{1}H NMR (300 MHz, d_6-DMSO): δ 10.73 (s, 1H), 8.86 (dd, J = 9.32, 4.51 Hz, 1H), 8.60 (bs, 2H), 8.51 (d, J = 5.69 Hz, 1H), 8.21 (d, J = 1.72 Hz, 1H), 7.94 (d, J = 8.54 Hz, 1H), 7.73 (d, J = 8.50 Hz, 1H), 7.44 (d, J = 2.40 Hz, 1H), 7.24 (d, J = 8.28 Hz, 1H), 7.18 (dd, J = 5.67, 2.52 Hz, 1H), 7.02 (d, J = 2.16 Hz, 1H), 6.97 (dd, J = 8.20, 2.37 Hz, 1H), 4.14−4.03 (m, 2H), 2.99−2.92 (m, 2H), 2.91−2.81 (m, 3H), 2.78 (d, J = 4.76 Hz, 3H), 2.18−2.06 (m, 1H), and 1.90−1.72 (m, 1H). LC-MS: m/z 499.4 $[M + H]^+$, 497.4 $[M - H]^-$ (FA).

General Procedure B2, Amide Bond Formation. 7-(2-Acetamidopyridin-4-yloxy)-1,2,3,4-tetrahydronaphthalene-2-carboxylic acid (1.00 mg, 3.06 mmol), DIPEA (1.60 mL, 9.19 mmol), and HATU (1.75 g, 4.60 mmol) were combined in DMF (30 mL), and the solution was stirred for 30 min. *tert*-Butyl [4-amino-2-(trifluoromethyl)benzyl]-carbamate (889 mg, 3.06 mmol) was added, and the resulting mixture was stirred overnight at room temperature. Water was added to the reaction mixture, and the resulting precipitate was isolated by filtration, washed well with water and hexane, and dried under vacuum. Purification by column chromatography (SiO_2, elution with 20−80% EtOAc in hexane) provided *tert*-butyl [3-{[((2*S*)-7-{[2-(acetylamino)pyridin-4-yl]oxy}-1,2,3,4-tetrahydronaphthalen-2-yl)carbonyl]amino}-5-(trifluoromethyl)benzyl]carbamate as an off white solid (1.21 g, 66%) ^{1}H NMR (300 MHz, $CDCl_3$): δ 8.20 (s, 1H), 8.05 (d, J = 6.1 Hz, 1H), 7.83

(s, 1H), 7.75−7.70 (m, 1H), 7.12 (d, J = 8.3 Hz, 1H), 6.90−6.79 (m, 2H), 6.71 (dd, J = 6.1, 2.3 Hz, 1H), 5.01 (s, 1H), 4.32 (d, J = 6.0 Hz, 1H), 3.14−2.85 (m, 4H), 2.84−2.60 (m, 2H), 2.21 (s, 3H), 2.17−2.12 (m, 1H), 2.02−1.92 (m, 1H), and 1.45 (s, 9H).

General Procedure C, *tert*-Butyl Carbamate Deprotection. *tert*-Butyl [3-{[((2*S*)-7-{[2-(acetylamino)pyridin-4-yl]oxy}-1,2,3,4-tetrahydronaphthalen-2-yl)carbonyl]amino}-5-(trifluoromethyl)benzyl]-carbamate (1.21 g, 2.02 mmol) was dissolved in a 4.0 M HCl in dioxane solution (10 mL), and the solution was stirred for 2 h. The mixture was concentrated in vacuo. Purification of the resulting residue by column chromatography (SiO_2, elution with 4−10% MeOH (with 2% NH_4OH) in DCM) provided a white solid. This solid was dissolved in DCM (10 mL), and 2.0 M HCl in Et_2O was added (2 mL). This mixture was stirred for 5 min and then concentrated in vacuo to give (2*S*)-7-{[2-(acetylamino)pyridin-4-yl]oxy}-*N*-[3-(aminomethyl)-5-(trifluoromethyl)phenyl]-1,2,3,4-tetrahydronaphthalene-2-carboxamide·2HCl (**5**) as a white solid (807 mg, 70%). ^{1}H NMR (300 MHz, d_6-DMSO, HCl salt): δ 11.23 (br s, 1H), 10.74 (s, 1H), 8.43 (s, 2H), 8.23 (d, 1H), 8.13−7.99 (m, 2H), 7.58 (s, 1H), 7.35 (s, 1H), 7.28−7.22 (m, 1H), 7.05−6.94 (m, 2H), 6.87−6.80 (m, 1H), 4.13−4.02 (m, 2H), 2.98−2.79 (m, 5H), 2.10 (s, 4H), and 1.79 (br s, 1H). LC-MS: m/z 499.7 $[M + H]^+$; 497.4 $[M - H]^-$ (FA). HRMS: m/z calcd for $C_{26}H_{25}F_3N_4O_3$ $([M + H])^+$, 499.19515; found, 499.195700.

5-Fluoro-3,4-dihydro-1,8-naphthyridin-2(1*H*)-one (11). Palladium acetate (341 mg, 1.52 mmol) and 4,5-bis(diphenylphosphino)-9,9-dimethylxanthene (1.76 g, 3.04 mmol) were added to a three-necked, round-bottomed flask, and the flask was purged three times with argon. Degassed 1,4-dioxane (240 mL) was added, and the mixture was stirred and degassed again with argon. To this solution was added a solution of 2-chloro-4-fluoropyridine (20 g, 152 mmol) in degassed 1,4-dioxane (120 mL), *tert*-butyl carbamate (19.6 g, 167 mmol), NaOH (8.88 g, 222 mmol), and degassed water (4.0 mL, 222 mmol). The resulting mixture was stirred at 100 °C. After 1.5 h, the reaction mixture was cooled to room temperature and filtered through a pad of Celite. The pad was washed well with dioxane, and the filtrate was concentrated under reduced pressure to dryness. The resulting solid was recrystallized from 2-propanol (∼250 mL) to give *tert*-butyl (4-fluoropyridin-2-yl)carbamate (**9**) as a pale yellow crystalline solid (25.65 g, 79.5% yield). ^{1}H NMR (400 MHz, d_6-DMSO): δ 10.10 (s, 1H), 8.26 (dd, J = 9.5, 5.6 Hz, 1H), 7.60 (dd, J = 12.3, 2.3 Hz, 1H), 6.95 (ddd, J = 8.3, 5.6, 2.3 Hz, 1H), and 1.47 (s, 9H). LC-MS: m/z 213 $[M + H]^+$ (FA).

An oven-dried, three-neck, round-bottomed flask equipped with an overhead stirrer, temperature probe, and addition funnel was charged with *tert*-butyl (4-fluoropyridin-2-yl)carbamate (31.8 g, 150 mmol), TMEDA (56.6 mL, 375 mmol), and THF (200 mL). The solution was cooled to −78 °C, and a solution of *n*-BuLi (2.50 M in hexane, 150 mL, 375 mmol) was added dropwise so that the reaction mixture temperature remained below −70 °C. The reaction mixture was stirred at −78 °C for 1 h, and a solution of I_2 (95.2 g, 375 mmol) in THF (160 mL) was added via addition funnel. The addition was controlled to keep the reaction mixture temperature below −70 °C, and the resulting mixture was stirred at −78 °C for 1 h. A solution of $NaHSO_4$ (61 g, 580 mmol) in water (200 mL) was added to the reaction mixture as it warmed to room temperature. Ethyl acetate was added, and the two-phase mixture was stirred at room temperature for 1 h. Water (500 mL) was added, and the phases were separated. The aqueous phase was extracted with EtOAc (3 × 400 mL), and the organic phases were combined, dried over $MgSO_4$, filtered, and concentrated to give an off white solid. This solid was suspended in DCM (50 mL), and the solid was isolated by filtration and washed with a minimum of DCM. The filtrate was concentrated and filtered to give a second crop of product. The solids were combined and dried under vacuum to give *tert*-butyl (4-fluoro-3-iodopyridin-2-yl)carbamate (**10**) as a white solid (45.63 g, 86% yield). ^{1}H NMR (400 MHz, d_6-DMSO): δ 9.47 (s, 1H), 8.32 (dd, J = 8.9, 5.5 Hz, 1H), 7.18 (dd, J = 7.2, 5.5 Hz, 1H), and 1.44 (s, 9H). LC-MS: m/z 339 $[M + H]^+$ (FA).

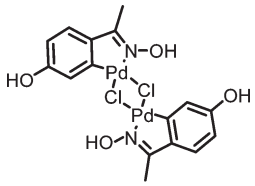

29

A round-bottomed flask was charged with *tert*-butyl (4-fluoro-3-iodopyridin-2-yl)carbamate (20.0 g, 59.2 mmol), 3,3-diethoxy-1-propene (13.5 mL, 88.7 mmol), DMF (150 mL), water (50 mL), DIPEA (15.4 mL, 88.7 mmol), and Pd catalyst **29**[21] (480 mg, 0.827 mmol), and the reaction mixture was warmed to 140 °C. After 5 h, the reaction mixture was cooled in a refrigerator for 2 days. The precipitate was isolated by filtration, washed with diethyl ether, and dried to give 3.25 g of pink needles. The filtrate was concentrated to give a reddish semisolid. This material was redissolved in DCM, and the solution was passed through 200 g of SiO_2. Concentration of the resulting solution provided a red/orange residue, which was recrystallized from 2-propanol (150 mL) to give 9.4 g of a pink solid. Purification of this pink solid by column chromatography (SiO_2, elution with 0−75% EtOAc/DCM) provided 1.41 g of a white powder. Overall, 4.66 g of 5-fluoro-3,4-dihydro-1,8-naphthyridin-2(1*H*)-one (**11**) was isolated (47% yield). ^{1}H NMR (400 MHz, d_6-DMSO): δ 10.7 (s, 1H), 8.11 (dd, J = 8.5, 5.7 Hz, 1H), 6.91 (dd, J = 8.8, 5.7 Hz, 1H), 2.91−2.85 (m, 2H), and 2.55−2.50 (m, 2H). LC-MS: m/z 167 $[M + H]^+$ (FA).

(2*S*)-*N*-[3-[(Isopropylamino)methyl]-5-(trifluoromethyl)-phenyl]-7-[(7-oxo-5,6,7,8-tetrahydro-1,8-naphthyridin-4-yl)oxy]-1,2,3,4-tetrahydronaphthalene-2-carboxamide (7). A mixture of 5-fluoro-3,4-dihydro-1,8-naphthyridin-2(1*H*)-one (**11**, 50.0 mg, 0.301 mmol), (2*S*)-7-hydroxy-1,2,3,4-tetrahydro-naphthalene-2-carboxylic acid [(*S*)-**15**, 63.6 mg, 0.331 mmol], cesium carbonate (294 mg, 0.903 mmol), and *N*,*N*-dimethylacetamide (1.40 mL) was combined. The mixture was sealed in a microwave vial and heated in the microwave at 150 °C for 1 h. Water (5 mL) was added, and the mixture was allowed to stir for a few minutes. The clear solution was then neutralized by the addition of 1 N HCl solution, and the resulting suspension was filtered through a Celite pad. The solid residue was washed with MeOH, and the filtrate was concentrated in vacuo. The residue was purified by column chromatography (SiO_2, eluting with 2−10% MeOH in DCM) to give (2*S*)-7-[(7-oxo-5,6,7,8-tetrahydro-1,8-naphthyridin-4-yl)oxy]-1,2,3,4-tetrahydronaphthalene-2-carboxylic acid (42 mg, 41% yield), ee 93.2% (ee determined by chiral HPLC, Column: IA 4.6 mm × 250 mm, eluting with 100/0.1 EtOH/TFA, at 0.5 mL/min for 50 min). ^{1}H NMR (400 MHz, d_6-DMSO): δ 11.94 (s, 1H), 10.10 (s, 1H), 7.57 (d, J = 5.8 Hz, 1H), 6.76 (d, J = 8.3 Hz, 1H), 6.54−6.44 (m, 2H), 5.89 (d, J = 5.8 Hz, 1H), 2.64−2.34 (m, 6H), 2.33−2.23 (m, 1H), 2.16−2.12 (m, 2H), 1.79−1.65 (m, 1H), and 1.42−1.28 (m, 1H).

(2*S*)-7-[(7-Oxo-5,6,7,8-tetrahydro-1,8-naphthyridin-4-yl)oxy]-1,2,3,4-tetrahydronaphthalene-2-carboxylic acid and *tert*-butyl [3-amino-5-(trifluoromethyl)benzyl]isopropylcarbamate were combined as described in General Procedure B2, Amide Bond Formation, and the Boc group was removed as described in General Procedure C, *tert*-Butyl Carbamate Deprotection, to give **7** as the HCl salt (67% yield over both steps). ^{1}H NMR (400 MHz, d_6-DMSO): δ 10.71 (s, 1H), 10.61 (s, 1H), 9.07 (s, 2H), 8.11 (s, 1H), 8.05 (s, 1H), 7.99 (d, J = 5.9 Hz, 1H), 7.68 (s, 1H), 7.19 (d, J = 8.3 Hz, 1H), 6.95−6.88 (m, 2H), 6.32 (d, J = 5.9 Hz, 1H), 4.22−4.17 (m, 2H), 3.38−3.28 (m, 1H), 3.01−2.75 (m, 7H), 2.54 (t, J = 7.7, 7.7 Hz, 2H), 2.16−2.07 (m, 1H), 1.88−1.72 (m, 1H), 1.30 (s, 3H), and 1.28 (s, 3H). HRMS: m/z calcd for $C_{30}H_{31}F_3N_4O_3$ $([M + H])^+$, 553.24210; found, 553.24265.

General Procedure B3, Amide Bond Formation. A solution of *N*-(4-{[(7*R*)-7-amino-5,6,7,8-tetrahydronaphthalen-2-yl]oxy}pyridin-2-yl)cyclopropanecarboxamide (10.2 g, 31.5 mmol) and HCl (2.0 M solution in Et_2O, 32 mL, 63 mmol) in pyridine (170 mL) was treated with 3-[(dimethylamino)methyl]-5-(trifluoromethyl)benzoic acid·Li salt (9.18 g, 36.3 mmol) and EDCI (9.67 g, 50.5 mmol). This solution was stirred overnight and then partitioned between EtOAc (500 mL) and half-saturated $NaHCO_3$ solution (500 mL). The aqueous phase was extracted with DCM (2 × 100 mL), and the combined organic phases were washed with brine, dried over Na_2SO_4, filtered, and concentrated. Purification by column chromatography (SiO_2, elution with 100% DCM to 15% EtOH, 15% MeCN, and 75% DCM) provided *N*-[(2*R*)-7-({2-[(cyclopropylcarbonyl)amino]pyridin-4-yl}oxy)-1,2,3,4-tetrahydronaphthalen-2-yl]-3-[(dimethylamino)methyl]-5-(trifluoromethyl)benzamide (**8**) as a beige powder (14.3 g, 82%).

General Procedure D, HCl Salt Formation. Compound **8** (14.3 g, 25.9 mmol) was dissolved in Et_2O (200 mL), and the solution was cooled to 0 °C. HCl (2.0 M in Et_2O, 39 mL, 78 mmol) was added dropwise over 10 min, and a precipitate appeared immediately. The mixture was warmed to room temperature and stirred for 15 min. The hygroscopic precipitate was isolated by filtration, redissolved in EtOH and MeOH, concentrated in vacuo, and dried in a vacuum oven at 37 °C overnight. Compound **8**·2HCl was provided as an off white solid (14.2 g, 88%). ^{1}H NMR (400 MHz, d_6-DMSO, HCl salt): δ 11.62−11.77 (m, 1H), 10.77 (s, 1H), 8.43 (br s, 2H), 8.22 (d, 1H), 8.06 (s, 1H), 8.03 (s, 1H), 7.59 (s, 1H), 7.33 (s, 1H), 7.24 (d, 1H), 7.04−6.95 (m, 2H), 6.88−6.82 (m, 1H), 4.05−4.11 (m, 2H), 2.99−2.75 (m, 5H), 2.17−1.72 (m, 3H), and 0.91−0.80 (m, 4H). LC-MS: *m*/*z* 525.6 $[M + H]^+$, 523.3 $[M - H]^-$ (FA). HRMS: *m*/*z* calcd for $C_{30}H_{31}F_3N_4O_3$ $([M + H])^+$, 553.24210; found, 553.242651.

General Procedure A2, Biaryl Ether Bond Formation. A mixture of (7*R*)-7-amino-5,6,7,8-tetrahydronaphthalen-2-ol hydrobromide (**17**, 16.7 g, 68.2 mmol), 5-fluoro-3,4-dihydro-1,8-naphthyridin-2(1*H*)-one (**11**, 11.36 g, 64.95 mmol), and cesium carbonate (63.49 g, 194.9 mmol) in DMF (216 mL) was stirred at 140 °C for 2 h. The reaction was not complete, so additional (7*R*)-7-amino-5,6,7,8-tetrahydronaphthalen-2-ol hydrobromide (**17**, 1.70 g, 6.82 mmol) was added. After an additional 1 h at 140 °C, the reaction mixture was cooled to room temperature and carefully treated with an aqueous 1 M HCl solution. The reaction mixture was then diluted with DCM and filtered through Celite. The phases were separated, and the aqueous phase was brought to pH 7 by the addition of a solution of NaOH (1.0 M). The brown precipitate was then removed by filtration through Celite, and the filtrate was washed with DCM. The aqueous phase was then brought to pH 14 by addition of a solution of NaOH (1.0 M), and an off-white precipitate formed. This suspension was treated with solid NaCl and stirred for 1 h. The solid was isolated by filtration and dried under vacuum to give 5-{[(7*R*)-7-amino-5,6,7,8-tetrahydronaphthalen-2-yl]oxy}-3,4-dihydro-1,8-naphthyridin-2(1*H*)-one as an off-white solid (17.7 g, 88% yield). ^{1}H NMR (400 MHz, d_6-DMSO): δ 10.6−10.4 (br s, 1H), 7.94 (d, *J* = 5.8 Hz, 1H), 7.13 (d, *J* = 7.9 Hz, 1H), 6.87−6.81 (m, 2H), 6.27 (d, *J* = 5.8 Hz, 1H), 3.05−2.96 (m, 1H), 2.93−2.79 (m, 4H), 2.77−2.66 (m, 1H), 2.55−2.50 (m, 2H), 2.46−2.38 (m, 1H), 1.92−1.84 (m, 1H), 1.82−1.60 (br s, 2H), and 1.51−1.40 (m, 1H). LC-MS: *m*/*z* 310 $[M + H]^+$ (AA).

3-[(Dimethylamino)methyl]-*N*-{(2*R*)-7-[(7-oxo-5,6,7,8-tetrahydro-1,8-naphthyridin-4-yl)oxy]-1,2,3,4-tetrahydronaphthalen-2-yl}-5-(trifluoromethyl)benzamide (26). 3-[(Dimethylamino)methyl]-5-(trifluoromethyl)benzoic acid·Li salt and 5-{[(7*R*)-7-amino-5,6,7,8-tetrahydronaphthalen-2-yl]oxy}-3,4-dihydro-1,8-naphthyridin-2(1*H*)-one were combined as described in General Procedures B3, Amide Bond Formation, and D, HCl Salt Formation, to provide **26** (20.9 g, 67%). ^{1}H NMR (400 MHz, CD_3OD): δ 8.36 (s, 1 H), 8.30 (s, 1H), 8.10−8.06 (m, 2H), 7.33−7.26 (m, 1H), 7.04−6.96 (m, 2H), 6.68 (d, *J* = 7.0 Hz, 1H), 4.51 (s, 2H), 4.40−4.31 (m, 1H), 3.24−3.16 (m, 3H), 3.06−2.94 (m, 3H), 2.90 (s, 6H), 2.81−2.77 (m, 2H), 2.26−2.19 (m, 1H), 2.01−1.89 (m, 1H). HRMS: *m*/*z* calcd for $C_{29}H_{29}F_3N_4O_3$ $([M + H])^+$, 539.22645; found, 539.22700.

3-(1-Amino-1-methylethyl)-*N*-{(2*R*)-7-[(7-oxo-5,6,7,8-tetrahydro-1,8-naphthyridin-4-yl)oxy]-1,2,3,4-tetrahydronaphthalen-2-yl}-5-(trifluoromethyl)benzamide (27). 3-{1-[(*tert*-Butoxycarbonyl)amino]-1-methylethyl}-5-(trifluoromethyl)benzoic acid and 5-{[(7*R*)-7-amino-5,6,7,8-tetrahydronaphthalen-2-yl]oxy}-3,4-dihydro-1,8-naphthyridin-2(1*H*)-one were combined as described in General Procedure B3, Amide Bond Formation, without the addition of HCl and General Procedure C to provide **27** (44.1 g, 61%). ^{1}H NMR (400 MHz, CD_3OD): δ 8.06 (s, 1H), 7.87 (s, 1H), 7.75 (d, *J* = 6.88 Hz, 1H), 7.67 (s, 1H), 6.95 (d, *J* = 8.40 Hz, 1H), 6.68−6.63 (m, 2H), 6.35 (d, *J* = 6.93 Hz, 1H), 4.05−3.95 (m, 1H), 2.88−2.81 (m, 3H), 2.70−2.58 (m, 3H), 2.45 (t, *J* = 7.46, 7.46 Hz, 2H), 1.91−1.83 (m, 1H), 1.67−1.55 (m, 1H), and 1.47 (s, 6H). HRMS: *m*/*z* calcd for $C_{29}H_{29}F_3N_4O_3$ $([M + H])^+$, 539.22645; found, 539.22700.

V600E and C-Raf Enzyme Assays. Raf enzyme activity was determined using a Flash Plate Assay format by adding 15 μL of a solution containing 50 mM HEPES, pH 7.5, 0.025% Brij 35, 10 mM DTT, and 10 nM Raf (^{V600E}ΔB-Raf or C-Raf) to the wells of an assay plate containing compound and was incubated for 20 min. A substrate solution (15 μL) containing 50 mM HEPES, pH 7.5, 0.025% Brij 35, 5 mM β-glycerol phosphate, 10 mM $MnCl_2$, 2 μM peptide (Biotin-DRGFPRARYRARTTNYNSSRSRFYSGFNSRPRGRVYRGRARATS-WYSPY-NH_2, New England Peptide), 1 μM ATP, 0.1 mg/mL BSA, and ^{33}P ATP 0.5 μCi/reaction was then added. The reaction mixture was incubated for 3 h and then stopped by the addition of 50 μL of 100 mM EDTA. The stopped reaction mixture (65 μL) was transferred to a Flash Plate (Perkin-Elmer) and incubated for 1 (C-Raf) or 2 (^{V600E}ΔB-Raf) h. The wells were washed three times with 0.02% Tween-20. Plates were read on a TopCount analyzer.

pERK Cell-Based Assay. Inhibition of Raf kinase activity in whole cells was assessed by determining the decrease in phosphorylation of the pERK, a kinase downstream of Raf, phosphorylated by MEK. A375 cells were seeded in a 96-well cell culture plate (12 × 103 cells/75 μL/well) and incubated overnight at 37 °C. Compounds were added, and cells were incubated with Raf kinase inhibitors for 3 h at 37 °C. Medium was removed, and cells were fixed with 4% paraformaldehyde for 15 min at room temperature. Four percent paraformaldehyde was replaced with methanol for a 15 min treatment and then blocked with 10% sheep serum and 1% BSA in PBS for 1 h. Cells were then incubated with anti-pERK antibody (1:100, Cell Signaling Technologies, #9101 L) (20 μL/well) overnight at 4 °C. After they were washed with PBS three times, the cells were stained with antirabbit horseradish peroxidase-linked antibody from donkey (1:100, Amersham Bioscience #NA9340) for 1 h at room temperature. Cells were washed three times with 0.5% Tween-20 in PBS and then three more times with PBS. 3,3′,5,5′-Tetramethylbenzidine liquid substrate system (50 μL/well) was added, and cells were incubated for 20−30 min at room temperature. The optical density was read at 650 nm. The cells were then washed 3−5 times with PBS to remove color solution. Results were normalized for the protein content in each well using a BCA protein assay kit (Pierce).

Xenograft Studies. The A375 M cell line (a derivative of A375[22]) was licensed from MD Anderson Cancer Center. Nude NCR (*nu*/*nu*) mice were purchased from Taconic. All animals were housed and handled in accordance with the Guide for the Care and Use of Laboratory Animals and Millennium Institutional Animal Care and Use Committee guidelines. Six to eight week old mice were inoculated subcutaneously with A375 M cells (5 × 10^6) in the right flank. Mice were dosed orally with 0.2 mL of **26** or **27** or vehicle only as a control. The vehicle was 10% (2-hydroxypropyl)-β-cyclodextrin (HPbCD) in

water, and the pH was adjusted to between 4 and 6 by the addition of 0.1 N NaOH.

For efficacy studies, mice were randomized to generate groups of 10 per treatment with equivalent average initial tumor volume (150−200 mm^3) and dosed daily for 21 days. Tumor volumes were measured twice a week using vernier calipers, and volumes were calculated using the formula $L \times W^2 \times 0.5$.

For PK/PD studies, mice were euthanized, and blood was collected by cardiac puncture and processed to plasma. Compound levels were measured in plasma by LC/MS/MS. Xenograft tumors were excised and trimmed of necrotic areas and flash-frozen for PD analysis. pERK levels were measured in tumor lysates by Li-Cor quantitative Western blot using a rabbit monoclonal antibody (pERK1/2-Thr202/Tyr204, Cell Signaling Catalog #4377).

■ ASSOCIATED CONTENT

Supporting Information. Synthetic details and characterization data for 7-(2-acetamidopyridin-4-yloxy)-1,2,3,4-tetrahydronaphthalene-2-carboxylic acid, *N*-(4-{[(7*R*)-7-amino-5,6,7,8-tetrahydronaphthalen-2-yl]oxy}pyridin-2-yl)cyclopropanecarboxamide, *N*-(4-nitropyridin-2-yl)-acetamide, *N*-(4-nitropyridin-2-yl)-cyclopropane-carboxamide, *tert*-butyl [3-amino-5-(trifluoromethyl)benzyl]isopropylcarbamate, 3-[(dimethylamino)methyl]-5-(trifluoromethyl)benzoic acid·Li salt, 3-{1-[(*tert*-butoxycarbonyl)amino]-1-methylethyl}-5-(trifluoromethyl)benzoic acid, and compounds **6**, (±)-**15**, (*S*)-**15**, **17**, and **19**−**25**; and kinase binding data for **26** and **27**. This material is available free of charge via the Internet at http://pubs.acs.org.

■ AUTHOR INFORMATION

Corresponding Author

*Tel: 617-761-6959. Fax: 617-551-8907. E-mail: sandy.gould@mpi.com.

■ ACKNOWLEDGMENT

We thank Ashok Patil and Nanda Gulavita for assistance in purification; Xiaofeng Yang for determining the exact masses; David Lok and Nina Molchanova for determining the HPLC purity of our compounds; Bi-Ching Sang, Garret Textor, Matt Kroeger, and Gyorgy Snell from Takeda San Diego for their assistance in determining the crystal structure of compound **24**; and Matt Jones, Ling Xu, David Lok, Susan Chen, and Shaoxia Yu for determining plasma levels of the compounds described in this paper. We also thank ALS, which is supported by the Director, Office of Science, Office of Basic Energy Sciences, Materials Sciences Division of the U.S. Department of Energy, under contract DE-AC03-76SF00098 at Lawrence Berkeley National Laboratory.

■ ABBREVIATIONS USED

MAPK, mitogen-activated protein kinase; ERK, extracellular signal-regulated kinase; MEK, mitogen-activated protein kinase; PK, pharmacokinetic; Clp, plasma clearance; Vss, steady state volume of distribution; AUC, area under the curve; HPbCD, (2-hydroxypropyl)-β-cyclodextrin; PK/PD, pharmacokinetic/pharmacodynamic; RTK, receptor tyrosine kinase

■ REFERENCES

(1) Robinson, M. J.; Cobb, M. H. Mitogen-activated Protein Kinase Pathways. *Curr. Opin. Cell Biol.* **1997**, *9*, 180–186.

(2) Roberts, P. J.; Der, C. J. Targeting the Raf-MEK-ERK mitogen-activated protein kinase cascade for the treatment of cancer. *Oncogene* **2007**, *26*, 3291–3310.

(3) Davies, H.; Bignell, G. R.; Cox, C.; Stephens, P.; Edkins, S.; Clegg, S.; Teague, J.; Woffendin, H.; Garnett, M. J.; Bottomley, W.; Davis, N.; Dicks, E.; Ewing, R.; Floyd, Y.; Gray, K.; Hall, S.; Hawes, R.; Hughes, J.; Kosmidou, V.; Menzies, A.; Mould, C.; Parker, A.; Stevens, C.; Watt, S.; Hooper, S.; Wilson, R.; Jayatilake, H.; Busterson, B. A.; Cooper, C.; Shipley, J.; Hargrave, D.; Pritchard-Jones, K.; Maitland, N.; Chenevix-Trench, G.; Riggins, G. J.; Bigner, D. D.; Palmieri, G.; Cossu, A.; Flanagan, A.; Nicholson, A.; Ho, J. W. C.; Leung, S. Y.; Yuen, S. T.; Weber, B. L.; Seigler, H. F.; Darrow, T. L.; Paterson, H.; Marais, R.; Marshall, C. J.; Wooster, R.; Stratton, M. R.; Futreal, P. A. Mutations of the BRAF Gene in Human Cancer. *Nature* **2002**, *417*, 949–954.

(4) Lee, J. H.; Lee, E.-S.; Kim, Y.-S. Clinicopathologic Significance of BRAF V600E Mutations in Papillary Carcinomas of the Thyroid. *Cancer* **2007**, *110*, 38–46.

(5) Gray-Schopfer, V.; Wellbrock, C.; Marais, R. Melanoma biology and new targeted therapy. *Nature* **2007**, *445*, 851–857.

(6) King, A. J.; Patrick, D. R.; Batorsky, R. S.; Ho, M. L.; Do, H. T.; Zhang, S. Y.; Kumar, R.; Rusnak, D. W.; Takle, A. K.; Wilson, D. M.; Hugger, E.; Wnag, L; Karreth, F.; Lougheed, J. C.; Lee, J.; Chau, D.; Stout, T. J.; May, E. W.; Rominger, Ch. M.; Schaber, M. D.; Lou., L.; Lakdawala, A. S.; Adams, J. L.; Contractor, R. G; Smalley, K. S. M.; Herlyn, M.; Morrissey, M M.; Tuveson, D. A.; Huang, P. S. Demonstration of a genetic therapeutic index for tumors expressing oncogenic BRAF by the kinase inhibitor SB-590885. *Cancer Res.* **2006**, *66*, 11100–11105. Tsai, J.; Lee, J. T.; Wang, W.; Zhang, J.; Cho, H.; Mamo, S.; Bremer, R.; Gillette, S.; Kong, J.; Haass, N. K.; Sproesser, K.; Li, L.; Smalley, K. S. M.; Fong, D.; Zhu, Y.-L.; Marimuthu, A.; Nguyen, H.; Lam, B.; Liu, J.; Cheung, I.; Rice, J.; Suzuki, Y.; Luu, C.; Settachatgul, C.; Shellooe, R.; Cantwell, J.; Kim, S.-H.; Schlessinger, J.; Zhang, K. Y. J.; West, B. L.; Powell, B.; Habets, G.; Zhang, C.; Ibrahim, P. N.; Hirth, P.; Artis, D. R.; Herlyn, M.; Bollag, G. Discovery of a selective inhibitor of oncogenic B-Raf kinase with potent antimelanoma activity. *Proc. Natl. Acad. Sci. U.S.A.* **2008**, *105*, 3041–3046. Yang, H.; Higgins, B.; Kolinsky, K.; Packman, K.; Go, Z.; Iyer, R.; Kolis, S.; Zhao, S.; Lee, R.; Grippo, J. F.; Schostack, K.; Simcox, M. E.; Heimbrook, D.; Bollag, G.; Su, F. RG7204 (PLX4032), a Selective BRAFV600E Inhibitor, Displays Potent Antitumor Activity in Preclinical Melanoma Models. *Cancer Res.* **2010**, *70*, 5518–5527. Joseph, E. W.; Pratilas, C. A.; Poulikakos, P. I.; Tadi, M.; Wang, W.; Taylor, B. S.; Halilovic, E.; Persaud, Y.; Xing, F.; Viale, A.; Tsai, J.; Chapman, P. B.; Bollag, G.; Solit, D. B.; Rosen, N. The RAF inhibitor PLX4032 inhibits ERK signaling and tumor cell proliferation in a V600E BRAF-selective manner. *Proc. Natl Acad. Sci. U.S.A.* **2010**, *107*, 14903–14908.

(7) Solit, D. B.; Garraway, L. A.; Pratilas, C. A.; Sawai, A.; Getz, G.; Basso, A.; Ye, Q.; Lobo, J. M.; She, Y.; Osman, I.; Golub, T. R.; Sebolt-Leopold, J.; Sellers, W. R.; Rosen, N. BRAF mutation predicts sensitivity to MEK inhibition. *Nature* **2006**, *439*, 358–362. Davies, B. R.; Logie, A.; McKay, J. S.; Martin, P.; Stelle, S.; Jenkins, R.; Cockerill, M.; Cartlidge, S.; Smith, P. D. AZD6244 (ARRY-142886), a potent inhibitor of mitogen-activated protein kinase/extracellular signal-regulated kinase kinase 1/2 kinases: mechanism of action in vivo, pharmacokinetic/pharmacodynamic relationship, and potential for combination in preclinical models. *Mol. Cancer Ther.* **2007**, *6* (8), 2209–2219.

(8) Bollag, G.; Hirth, P.; Tsai, J.; Zhang, J.; Ibrahim, P. N.; Cho, H.; Spevak, W.; Zhang, C.; Zhang, Y.; Habets, G.; Burton, E. A.; Wong, B.; Tsang, G.; West, B. L.; Powell, B.; Shellooe, R.; Marimuthu, A.; Nguyen, H.; Zhang, K. Y. J.; Artis, D. R.; Schlessinger, J.; Su, F.; Higgins, B.; Iyer, R.; D'Andrea, K.; Koehler, A.; Stumm, M.; Lin, P. S.; Lee, R. J.; Grippo, J.; Puzanov, I.; Kim, K. B.; Ribas, A.; McArthur, G. A.; Sosman, J. A.; Chapman, P. B.; Flaherty, K. T.; Xu, X.; Nathanson, K. L.; Nolop, K. Clinical efficacy of a RAF inhibitor needs broad target blockade in BRAF-mutant melanoma. *Nature* **2010**, *467*, 596–599. Flaherty, K.; Puzanov, I.; Sosman, J.; Kim, K.; Ribas, A.; McArthur, G.; Lee, R. J.; Grippo, J. F.; Nolop, K.; Chapman, P. Phase I study of PLX4032: Proof of concept for V600EBRAF mutation as a therapeutic target in human

cancer. *J. Clin. Oncol. (Meeting Abstr.)* **2009**, *27*, 9000. (c) Wellbrock, C.; Hurlstone, A. BRAF as therapeutic target in melanoma. *Biochem. Pharmacol.* **2010**, *80*, 561–567.

(9) Sorafenib (**1**) is a multikinase inhibitor with modest inhibitory activity against Raf. This compound has shown efficacy in the clinic and is now marketed as Nexavar. Wilhelm, S. M.; Carter, C.; Tang, L.; Wilkie, D.; McNabola, A.; Rong, H.; Chen, C.; Zhang, X.; Vincent, P.; McHugh, M.; Cao, Y.; Shujath, J.; Gawlak, S.; Eveleigh, D.; Rowley, B.; Liu, L.; Adnane, L.; Lynch, M.; Auclair, D.; Taylor, I.; Gedrich, R.; Voznesensky, A.; Riedl, B.; Post, L. E.; Bollag, G.; Trail, P. A. BAY43-9006 exhibits broad spectrum oral antitumor activity and targets the RAF/MEK/ERK pathway and receptor tyrosine kinases involved in tumor progression and angiogenesis. *Cancer Res.* **2004**, *64*, 7099–7109. Adnane, L.; Trail, P. A.; Taylor, I.; Wilhelm, S. M. Sorafenib (BAY43-9006, Nexavar), a dual-action inhibitor that targets RAF/MEK/ERK pathway in tumor cells and tyrosine kinasese VEGFR/PDGFR in tumor vasculature. *Methods Enzymol.* **2006**, *407*, 597–612.

(10) Bankston, D.; Dumas, J.; Natero, R.; Riedl, B.; Monahan, M. K.; Sibley, R. A Scaleable Synthesis of BAY43-9006: A Potent Raf Kinase Inhibitor for the Treatment of Cancer. *Org. Process Res. Dev.* **2002**, *6*, 777–781 Riedl, B.; Dumas, J.; Khire, U.; Lowinger, T. B.; Scott, W. J.; Smith, R. A.; Wood, J. E.; Monahan, M.-K.; Natero, R.; Renick, J.; Sibley, R. N. U.S. Patent 7 235 576 B1, 2007.

(11) Calderwood, E. F.; Duffey, M.; Gould, A. E.; Greenspan, P. D.; Kulkarni, B.; Lamarche, M. J.; Rowland, R. S.; Tregay, M.; Vos, T. J. PCT Int. Appl. WO 2007067444 A1 20070614, 2007.

(12) Xi, N.; Hale, C.; Kelly, M. G.; Norman, M. H.; Stec, M.; Xu, S.; Baumgartner, J. W.; Fotsch, C. Synthesis of novel melanocortin 4 recpetor agonists and antagonists containing a succinamide core. *Bioorg. Med. Chem. Lett.* **2004**, *14*, 377–381.

(13) Van Heerden, P. S.; Bezuidenhoudt, B. C. B.; Ferreira, D. Efficient Asymmetric Synthesis of the Four Diastereomers of Diphenacoum and Brodifacoum. *Tetrahedron* **1997**, *53* (17), 6045.

(14) The opposite enantiomer can be prepared by employing the opposite enantiomer of the Evans' auxiliary.

(15) Boigegrain, R.; Cecchi, R.; Boveri, S. U.S. Patent 5 159 103, 1992.

(16) Hirayama, Y.; Ikuaka, M.; Matsumoto, J. An Expeditious Scalable Synthesis of (S)-2-Amino-5-methoxytetralin via Resolution. *Org. Process Res. Dev.* **2005**, *9*, 30–38.

(17) Wan, P. T. C.; Garnett, M. J.; Roe, M. S.; Lee, S.; Niculescu-Duvaz, D.; Good, V. M.; Jones, M. J.; Marshall, C. J.; Springer, C. J.; Barford, D.; Marais, R. Mechanism of Activation of the RAF-ERK Signaling Pathway by Oncogenic Mutations of B-RAF. *Cell* **2004**, *116*, 855–867.

(18) Gould, A. E.; Harrison, S. J.; Mizutani, H.; Shen, M.; Smyser, T. E.; Stroud, S. G. U.S. Patent Appl. US 20100197924 A1 20100805, 2010.

(19) Additional kinase binding data for **26** and **27** can be found in the Supporting Information, Table 1.

(20) Crystallization work was done with wt B-Raf protein (residues 445−726). The crystallization conditions were as follows: 14.025% PEG 8000, 0.8 M NP Lithium Cl, 0.06 M Tris base, and 0.04 M Tris Cl. A 50 mM stock concentration of compound was made in 100% DMSO. The compound (50 mM) was mixed with B-raf (2.64 mg/mL) to a final concentration of 1 mM compound at room temperature. The precipitate was removed by centrifugation. The crystals appeared after 7 days. Crystals were frozen by flash freezing in liquid nitrogen using 25% ethylene glycol in mother liquor. The crystals diffracted to 3.1 Å, and clear omit electron density for the compound was observed. The data collection summary and refinement statistics have been deposited in the RCSB Protein Data Bank (RCSB ID code rcsb063351 and PDB ID code 3Q96).

(21) Corma, A.; Garcia, H.; Leyva, A. Comparison between polyethylenglycol and imidazolium ionic liquids as solvents for developing a homogeneous and reusable palladium catalytic system for the Suzuki and Sonogashira coupling. *Tetrahedron* **2005**, *61*, 9848–9854.

(22) Li, L.; Price, J. E.; Fan, D.; Zhang, R. D.; Bucana, C. D.; Fidler, I. J. Correlation of growth capacity of human tumor cells in hard agarose with their in vivo proliferative capacity at specific metastatic sites. *J. Natl. Cancer Inst.* **1989**, *81*, 1406–1412.